



Modelling and experimental design of a stagnant film crystalliser for freezing desalination treatment of seawater using sweating steps and non-direct freezing

Rusul Naseer Mohammed^{a,*}, Saad Abu-Alhail^b, Ahmed Naseh Ahmed Hamdan^b

^aDepartment of Chemical Engineering, College of Engineering, University of Basra, Basra City, Iraq, Tel. +964 (0) 78 26 64 80 032; email: rusalsaad@yahoo.com

^bDepartment of Civil Engineering, College of Engineering, University of Basra, Basra City, Iraq

Received 16 March 2017; Accepted 14 November 2017

ABSTRACT

A stagnant film crystalliser for the treatment of seawater by a combination of freezing and sweating steps using non-direct freezing, so-called PNDF, was developed. All tests were carried out with samples of seawater from the Gulf near Fao, Basra, Iraq. The pilot plant consists of a cooling cylinder. The crystallisation tubes are located in a cylinder-shaped paired jacketed tank refrigerated via a thermostatic bath. The effects of the main parameters on the sweating steps including the sweating rate, initial concentration of frozen water, sweating temperature, and sweating time were examined. The experimental design used to study the influence of these parameters limits the weight of the purified frozen product. The weight loss of frozen water increased with increasing sweating rate, from 0.0089 to 0.05 K/min, whereas the weight loss was almost unaffected by the purity of the initial frozen water film. A statistical model was built and calibrated to the experimental data to evaluate the experimental strategy and predict the purity of the frozen water using three sodium chloride concentrations 5.33, 7.42, and 14.92 mg/L. The demonstration of the statistical model enabled the selection of the optimal running time, resulting in the production of 0.4 g/kg pure water (less than the standard value of drinking water) in one stage within 29 h. The results obtained with seawater sampled near the port of Fao, Iraq, showed that PNDF can reduce the total dissolved solids to 0.3% of 41,750 mg/L with 96% recovery without using chemical additives; furthermore, chloride removal was 85%.

Keywords: Freezing; Saline water treatment; Crystallisation

1. Introduction

The freezing of saline water results in the formation of ice crystals. This occurs when temperature of the saline water becomes lower than its freezing point [1]. The freezing involves a change from the liquid phase to the solid phase, which becomes a different phase on distillation. Ice liquid refrigerants are treated with saltwater in a freezer distiller where the vaporisation of the refrigerant absorbs the heat from the saltwater, allowing it to freeze. Several freezing distillation methods have been used depending on the process requirements including melting, re-forming, and freezing, which

have resulted in high energy efficiency [2]. There are different kinds of freezing methods, including eutectic separation, direct freezing, vacuum freezing, and non-direct freezing [3]. Direct freezing is the formation of water crystals using a refrigerant and saline water. In non-direct freezing, crystals are produced by circulating the refrigerant through a heat exchanger, resulting in a temperature decrease through conduction [5]. In comparison with other water treatment methods, freezing has many advantages such as its energy consumption; that is, for water, the latent heat of freezing is one-seventh of that of the latent heat of evaporation [4]. In addition, corrosion is reduced because of the low temperatures and toxic material

* Corresponding author.

is not produced [5,6]. However, there are some disadvantages of the freezing process, such as the increase in capital cost and the persistent and fundamental properties of the water [7,8]. Recently, several industrial applications using freezing have been demonstrated, such as the treatment of wastewater sludge [9–11], desalination, freezing/membrane desalination hybrids, and the absorption of fruit juice and dairy foods [12,13]. In addition, freezing can be used as a pre-treatment technique for the further treatment of saline water by reverse osmosis (RO) and electrodialysis [14]. In the past decades, several pilot plants have been developed that use the freezing treatment method in cold and remote regions. Nevertheless, the freezing method has not been used to yield drinking water commercially [15]. In a pilot industrial plant, it is expected that the static freezing approach is more efficient in reducing the energy consumption, as well as being more cost-effective; however, this method yields lower removal efficiencies for the preparation of potable water. However, this inefficiency can be avoided by sweating the frozen water film after the crystallisation step [16]. Thus, in this study, we aimed to develop a static film crystalliser by combining the freezing and sweating steps using non-direct freezing. Most of the experiments were carried out with an initial solution consisting of water and sodium chloride. The aim of this research is to determine the efficiency of PNDF for treating seawater from Fao, Iraq, to identify, using a statistical design method, the optimal working factors for producing drinkable water (less than 0.5 g/kg sodium chloride), and to predict the purity of frozen water using the statistical model.

2. Materials and methods

2.1. Analytical methods

This work was carried out using two types of solutions: seawater and synthetic seawater (sodium chloride solution). Four seawater samples were taken from different locations near the port of Fao (near Basra, Iraq) and tested according to APHA standard methods [17]. Each sample volume was 100 L. Frozen water samples were obtained from the film formed on the refrigerant tube surface and placed in an isothermal bathwater. Then, the samples were quickly cooled to 258.15 K (−15°C) for examination and observation. First, each sample was fixed on a copper support and pressed down by a microtome to achieve a smooth internal surface of the frozen water film. Saline water (sodium chloride solutions) was selected by measuring the weight of a dry sample of known weight, prepared by dehydration in an oven at 353.15 K (80°C) for 720 min. The flowchart of the freezing cycles before the sweating step is shown in Fig. 1.

2.2. Lab experiments

Fig. 2 shows a schematic of the equipment. The main part of the experimental equipment consists of a stainless-steel tube inside a 1-L glass beaker. The diameter of the tube was 5 cm. The effective tube length exposed to the frozen water was 50 cm. The freezing takes place at the edge of the beaker. A temperature of the coolant fluids circulating in the cylinder was adjusted using a temperature controller bath (1), and a second temperature controller controlled the temperature of

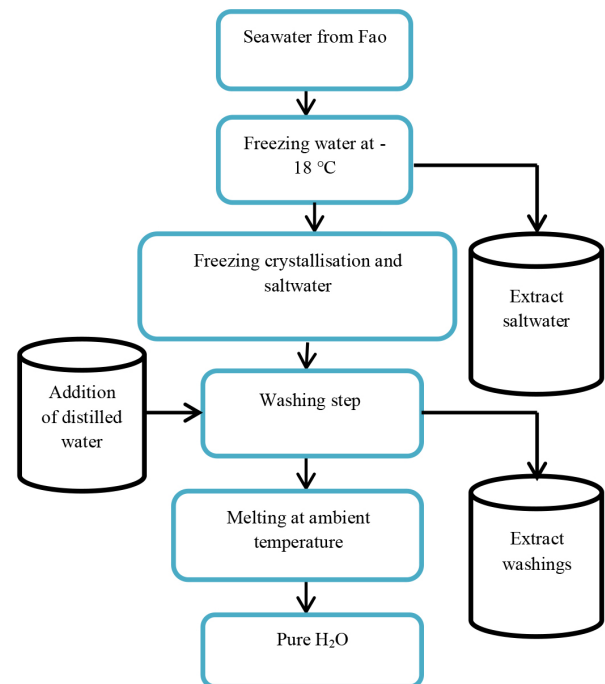


Fig. 1. Flow diagram of the freezing process before sweating step.

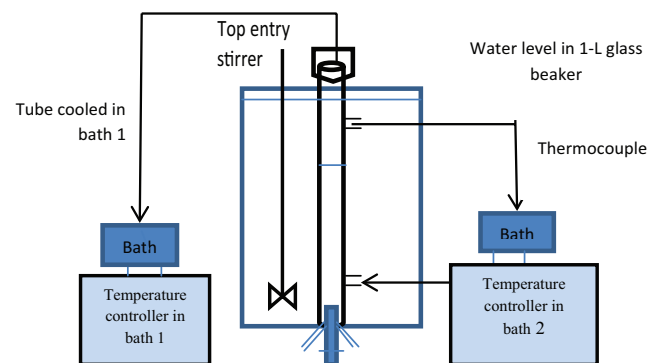


Fig. 2. Experimental setup of the sweating non-direct freezing (PNDF) plant.

the beaker (2). Standard Pt100 zero-temperature probes were used. After calibration, an accuracy of 0.05°C was achieved in the temperature domain of 253.15 to 269.15 K (−20°C to −4°C). The fixed part of the cylinder was covered with Teflon to avoid crystallisation and edge effects. Gravimetric analysis was used to select the salinities of various solutions. The dry extract from 1 mL of saline solution was prepared by drying in a test lab oven at 375 K for 720 min.

2.3. Experimental procedure

Saline water was introduced into the glass tank and pre-cooled using the thermostatic steam bath (marked 2 in Fig. 2). Freezing was carried out at the external layer of the cylinder. At the bottom, the cylinder was enclosed with Teflon to prevent crystallisation. It is important to produce

a covering of seed ice crystals on the cooling surface before placing the rod-shaped tube into the tank. If this step is omitted, a high degree of refrigeration is required to achieve crystallisation, which results in an increase in the initial growth rate and a polluted frozen water film. The crystallisation procedure was carried out by refrigerating the cylinder at 265.15 K (−8°C) in the first stage. Then, the tube was charged into the pure water to produce the frozen film (about 1 mm thick) on the external surface of the cylinder. After that, this layer was introduced in the beaker containing seawater and the cylinder was refrigerated to achieve crystallisation. This stage was carried out by decreasing the refrigeration temperature in the glass column from 274.65 to 268.05 K (1.5°C to −5.1°C) using a thermostatic steam bath (marked 1 in Fig. 2). The weight of the frozen water layer formed was about 0.1 kg. Different saline concentrations were investigated (between 15.3 and 2.5 g/kg) at different cooling rates, as shown in Table 1. Some of the residual solution was withdrawn from the bottom as the temperature of the cylinder tube was increased to the final crystallisation temperature. In the parametric study of the crystallisation step, the ice surface was washed by leaving the ice layer in the air at ambient temperature for 10 min. The ice surface slightly melted and the solution was recovered.

2.4. Sweating step

The refrigerant liquid inside the glass column was used to select the optimal sweating temperature. Then, the temperature was suddenly increased from the high crystallisation temperature to the optimal temperature. Most of the experiments were conducted at a constant temperature (T_p) over the whole sweating step (PR = 0). The jacketed wall temperature adjusts from a datum point of 273 K for all phases. The brine was drained, weighed, and collected to examine its salinity. At the end of the sweating step, the remaining frozen water film was liquid.

3. Results and discussion

3.1. Features investigation of the sweating step

The effects of important factors including the sweating rate (K/min), the initial concentration of the saline water (g/kg), and the final sweating temperature were investigated. Three frozen water concentrations (15.23, 3.92, and 7.41 g/kg) were sweated by adjusting the cylinder temperature from 268.33 to 274.85 K.

Table 1
Freezing conditions

Frozen water concentration (g/kg)	Refrigeration rate (K/min)	Running time (min)
15.23	0.516	180
9.1	0.162	780
7.23	0.114	1,080
5.61	0.102	1,380
3.92	0.06	1,680

3.1.1. Influence of sweating rate

The sweating rates tested were 0.042, 0.02, and 0.0089 K/min for 3, 6, and 9 h, respectively. Fig. 3 shows that the purity of the sweated frozen water increased with decreasing sweating rate. Thus, the weight loss was almost unchanged in the purer frozen water layer. Because the purity was higher at a lower sweating rate, this unchanged mass loss suggests that the sweating of purer frozen water is more efficient at a low rate. Clearly, the purity improved with increasing weight loss. The results show that the ice concentration decreased from 6.42 mg/L at 0.04 K/min to 3.8 mg/L at 0.0089 K/min sweating rate. Thus, the purity of the sweated frozen water increased with decreasing sweating rates for the three types of frozen water. As shown in Fig. 4, increasing the weight loss improved the purity. That is, the weight loss at a high salinity (15.38 g/kg) was greater than that at a low salinity (2.8 mg/L). Notably, the ice purity was higher when the initial frozen water film was purer.

3.1.2. Influence of the sweating temperatures

Fig. 5 shows the typical phase diagram for a two-component sodium chloride solution of 0.05 mol, which is the salinity of the seawater near Fao. When the temperature decreased below the freezing point, water begins to

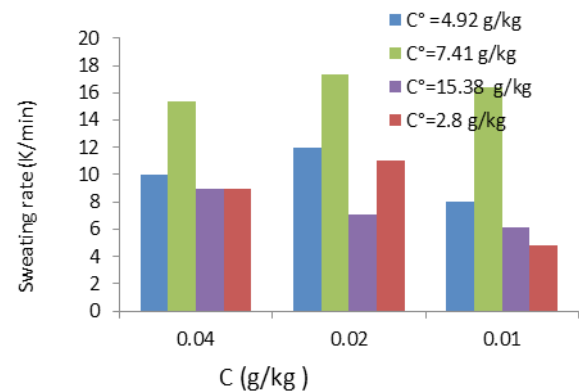


Fig. 3. Influence of sweating rate on ice purity.

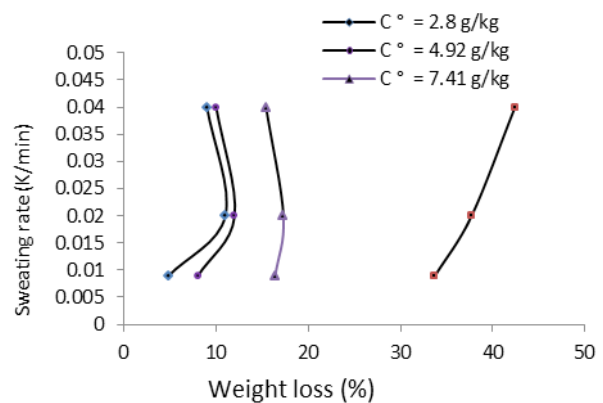


Fig. 4. Influence of sweating temperature on the purity of frozen water.

change from the liquid to the solid phase. During the transition, the normal freezing of water results in improved water purity [18,19] because salts are excluded from the solid state. In runs 1 and 2, the sweating rate gradually decreased from 0.04 to 0.00 K/min, and the temperature was fixed at 274.85 K. In run 3, the temperature was increased to 276.2 K and the sweating rate was set to 0.00 K/min. The result explains why the final frozen purity improved when the sweating temperature is 274.85 K and increasing the sweating temperature is of no benefit. As a result, the final temperature (274.85 K) is the most important parameter. This can be confirmed by a comparison of the results shown in Figs. 3 and 6. Indeed, a sweating period of 3 h is essential for an initial concentration of 2.8 g/kg, and a sweating period of 5 h is necessary for an initial frozen water concentration of 4.92 g/kg. A time of 9 h is compulsory for initial frozen water concentrations of 7.41 g/kg. A concentration of 15.38 g/kg is required to achieve the same purity, which was held at 274 K for the same period. In addition, increasing the sweating temperature during run 3 led to improved purity. Fig. 4 shows that the weight loss reached more than 60% at a high

temperature. Thus, a high temperature leads to more product with greater purity.

3.2. Setup strategy

Table 2 shows the parametric values of the factors for the experimental design in different phases. There are three

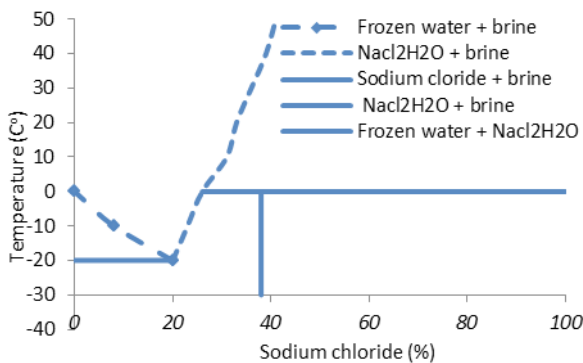


Fig. 5. Typical phase diagram of two-component saltwater solution.

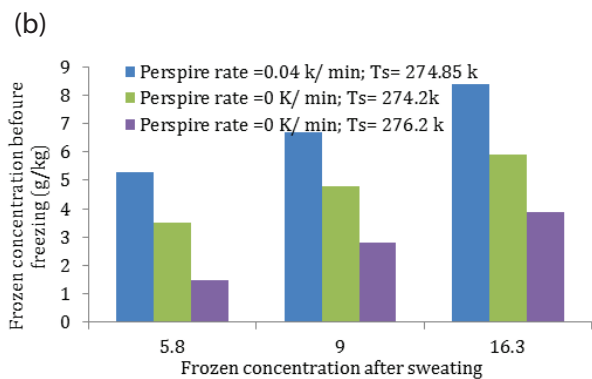
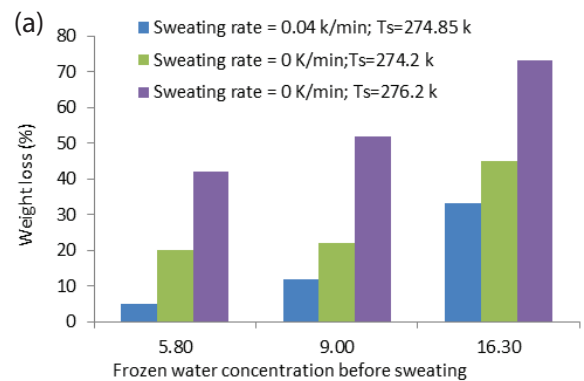


Fig. 6. Influence of sweating rate on weight loss.

Table 2
Parametric values for the experimental strategy

Phase	$C_{initial}$ (g/kg)	C_{after} (g/kg) ^a	C_r (g/kg) ^b	Sweating rate (K/min)	T_p (K)	Time (h)		$M_{freezing}$ (g)	M_r ^c (g)
						t_p	t_c		
I	15.23	4.94	50.3	0.042	274.85	3	6	85.03	190.21
II	15.23	3.12	49.8	0.0089	274.85	9	6	76.41	194.37
III	15.23	2.09	50.2	0.042	276.22	3	6	61.64	190.42
IV	15.23	0.43	50.4	0.0089	276.22	9	6	33.23	192.51
V	4.92	3.96	54.4	0.0042	274.85	3	25	69.51	189.45
VI	4.92	3.06	54.1	0.0089	274.85	9	25	55.92	192.65
VII	4.92	1.10	52.89	0.0042	276.22	3	25	67.41	191.89
VIII	4.92	0.21	52.13	0.0089	276.22	9	25	52.56	191.54
IX	7.41	2.54	85.4	0.021	274.85	6	15	75.53	192.91
X	7.41	2.11	84.2	0.021	274.85	6	15	76.93	190.54
XI	7.41	2.23	83.4	0.021	276.22	6	15	75.74	192.44
XII	7.41	1.24	82.1	0.0089	276.22	9	15	60.23	192.22

^aFrozen weight after sweating (g/kg).

^bResidual liquid weight.

^cWeight of residual crystallisation liquid.

T_p , sweating temperature; t_p , sweating time; t_c , crystallisation time.

variables recognised at each level: sweating rate, sweating temperature, and sweating time. An experimental design was chosen using four factors carried out in eight experiments. However, a different setup was repeated at the domain centre to calculate the coefficient of determination (R^2). The initial fluoride range was between 4.92 and 15.23 g/kg, which was selected depending on crystallisation runs to identify the optimal operating conditions. The results showed that the frozen film became fragile and could drop from the external column surface at a temperature greater than 274.4 K. At a high initial concentration of 15.23 g/kg, the weight and brine concentration after crystallisation are very similar in phases I, II, and III. In addition, the weight and the concentration are very similar in phases V, VI, and VII at 4.92 g/kg. However, the brine concentrations and mass decreased during phases V, VIII, and XII to less than 0.3 g/kg and 50 g, respectively. This is due to the lower sweating rate (0.0089 K/min) and higher sweating temperature (276.2 K).

3.3. Data analysis and optimisation

The Statgraphics software was used to analyse the experimental data. The program calculated the regression, effect of estimated variables, and response plotting. The fitting equation was determined after eliminating unimportant effects. For the frozen water concentration, the fitted equation is shown in Eq. (1), where the mean error equal is 0.091 and the correlation (R^2) is 98.55%.

$$C_i = 574.4 + 0.4346C^\circ - 2.08125T_p + 0.0665152 \times 3 - 0.0303 \times t_p \times C^\circ - 0.012303 \times C^\circ \times t_p \tag{1}$$

Here C° is the frozen water concentration before sweating in g/kg; C_i is the frozen water concentration after sweating in g/kg.

For the frozen weight, the fitted equation is shown in Eq. (2), where the mean error is equal to 2.7 with a correlation factor R^2 of 97.55%:

$$M_{\text{freezing}} = 5280.2 - 0.342C^\circ - 22.30T_p + 677.187t_s - 2.13 \times T_p \times t_p \tag{2}$$

The effects of all parameters on the purity of the frozen water and frozen weight are shown in Table 2. It was found that higher freezing purities after sweating occurred at lower initial frozen water concentrations with a higher temperature (276 K) and sweating times, as discussed in section 3.1. In addition, a high frozen weight after sweating (M_{freezing} greater than 80 g) was obtained with lower parameters.

A contour design was performed to determine the optimal operating parameters of the process. A frozen water concentration of less than 0.4 g/kg conforms to drinking water requirements with a reduction in the sweating period. Figs. 7(a) and (b) show the exterior response after carrying out sweating with two feed fluoride concentrations ($C^\circ = 15.23$ and 4.92 g/kg). The maximum temperature range was increased to 274.85 K. Four values for the experimental design were selected for validation of the model, as shown in Table 4. As shown, the working factors are different between the experimental design and the models. However, the working factors are within the range used to form the models where the two points are related to a final salinity of 0.4 g/kg. The result showed the final frozen mass values agreed with the value obtained from experiment, which is also shown as the root mean square error. It showed there is a good agreement between the final frozen water concentration and that predicted by design Eq. (1). As shown in the contour plots (Figs. 7(a) and (b)) the necessary sweating time is the lowest at higher temperatures. However, the frozen film can drop off the column layer if the sweating temperature is more

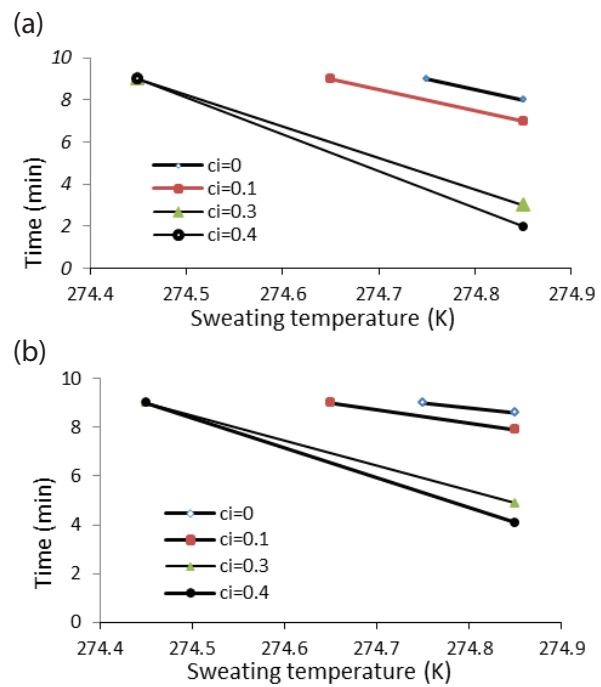


Fig. 7. Estimated surface responses. (a) $C^\circ = 14.92$ g/kg and (b) $C^\circ = 4.92$ g/kg.

Table 3 Evaluation of the experimental design

C_{initial} (g/kg)		C_{after} (g/kg) ^a		Sweating rate (K/min)		T_p (K)		t_p (h)		T_c (h)		M_{freezing} (g)	
Exp	Model	Exp	Model	Exp	Model	Exp	Model	Exp	Model	Exp	Model	Exp	Model
4.92	4.92	0.51	0.43	0.042	0.042	274.85	274.85	4.5	4.5	24	24	43.3	53.5
14.92	14.92	0.49	0.52	0.042	0.042	274.81	274.81	9	9	15	15	39.7	33.5
7.41	7.41	0.50	0.44	0.042	0.042	274.82	274.85	6.5	6.5	20	20	42.8	51.7

^aFrozen weight after sweating (g/kg).

than 274.4 K. Therefore, for $C^\circ = 4.92$ and 14.92 g/kg, the optimal temperature is 274.14 K. Notably, periods of 5 and 2 h result in a final salinity of 0.4 g/kg.

3.4. Evaluation of experimental designs

The chosen best values are points 1, 2, and 3 for the evaluation of the frozen water in the model. Table 3 shows the evaluation of the experimental design. It was selected to reduce the sweating rate, which reduces the energy consumption. In addition, the minimum time of crystallisation and the sweating time are defined as the whole desalination time. The total times were 31, 24, and 29 h for points 1, 2, and 3, respectively. The result showed that it is best to give a higher weight to the time in order to increase the efficiency. However, the energy consumption was increased by prolonging the crystallisation time. Thus, the initial concentration of 7.41 g/kg is a better value, and the sweating was achieved in one step. However, although the weight loss is increased by sweating, use of one step would reduce the operational costs to a greater extent than using two steps.

3.5. Comparison study

Table 4 shows the chemical and physical properties of the seawater from the port of Fao before and after the PNDF treatment. After the freezing had been carried out, the total dissolved salt (TDS) reduced to 1,108, 1,461, and 1,345 mg/L for tests 1, 2, and 3, respectively.

As shown in Fig. 8, the overall removal efficiency of all tests was in the range of 95%. Notably, all three tests presented a significant decrease in the amount of salt. Based on the 50-L test water volume, the chloride ion concentrations were reduced by 83%, 83%, and 85% for tests 1, 2, and 3, respectively. After PNDF had been carried out, the TDS decreased by 76%, 79%, and 77%, producing acceptable drinking water. The electrical conductivity decreased by 66%, 69%, and 68% for tests 1, 2, and 3, respectively.

Table 5 shows a comparison of different water purification methods [20–22]. Electrodialysis can treat water with a low concentration of total dissolved solid (less than 3,000 mg/kg). A high-quality water with lower energy consumption is produced by RO. The energy consumption in the RO method is currently about 3–4 kW/m³ when the equipment running at 40%–45% water recovery. The high-energy consumption results from the high-pressure reject stream [23]. The average power consumed by the high-pressure pump in parametric evaluation of energy consumption and loss in this equipment using energy recovery procedures is between 5.56 and 7.93 kW h/m³ [24]. Saline water RO with energy recovery consumes 5.2 kW/m³ electricity [25,26]. Thus, the energy consumption of the sweating PNDF process is high, and, although the new (PNDF) is simple, further development is essential for the reduction in energy loss. In addition, the total dissolved solids of the seawater from Fao used in this study is high (TDS 37,150 mg/L), which affects the energy loss significantly.

4. Conclusion

In the present study, the viability of the desalination of seawater from Fao (TDS 41,750 mg/L) was investigated

Table 4
Composition of seawater samples from Fao before and after PNDF

Test No.	Volume (L)		Cl ⁻ (mg/L)		HCO ₃ ⁻ (mg/L)		SO ₄ ⁻² (mg/L)		Mg ⁺² (mg/L)		Na ⁺ (mg/L)		K ⁺ (mg/L)		Ca ⁺² (mg/L)		Electrical conductivity (µS/cm)		Turbidity (mg/L)		Total dissolved salt (mg/L)	
	B	A	B	A	B	A	B	A	B	A	B	A	B	A	B	A	B	A	B	A	B	A
1	50	0.5	15,315	416	166.9	5	3,541	199	876	99	19,879	201	366	35	501	61	52,001	2,180	4,680	311	36,790	1,108
2	50	0.93	17,822	467	185	9	3,750	267	856	102	11,478	225	495	54	551	69	57,120	2,912	5,302	498	41,750	1,311
3	50	0.4	15,782	467	145	4	3,004	213	782	91	9,112	230	186	32	324	51	46,108	2,550	4,189	519	32,350	1,245

Note: Here, B means before the sweating step in PNDF and A means after the sweating step in PNDF.

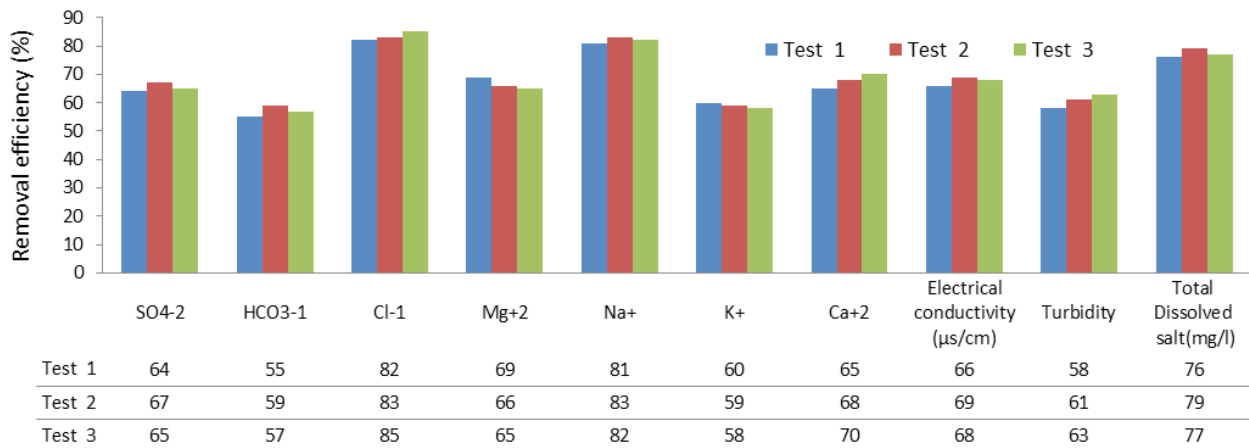


Fig. 8. Average removal efficiency for three tests of seawater from Fao.

Table 5
Comparison of different water purification methods

Method	Power (kW h/m ³)	Total dissolved solids (mg/L)
Electrodialysis	1	100–3,000
Reverse osmosis	0.4–0.7	1,000–45,000
Multi-stage flash (MSF) distillation	35	30,000–100,000
PNDF in this study	450	47,650–100,000

by a combination of the freezing and sweating steps using PNDf. The main operating parameters affecting the freezing were examined using a static film crystalliser. The sweating step can complete the desalination successfully. It was optimised to produce potable drinking water with a high removal efficiency. The purity of the frozen water film is intensely dependent on the solution mass. The frozen water is contaminated by liquid attachments containing frozen impurities, and increasing the brine salinity results in a reduction in the purity of the frozen water. The results demonstrate the feasibility of PNDf and can be used for its further optimisation. An experimental design used to investigate the influence of optimum running parameters on the purified frozen film weight and the sweating step. A statistical model was built and calibrated using the experimental data at different initial frozen water concentrations to evaluate the experimental strategy and for the prediction of the purity of the frozen water. As a final engineering observation, the development of freezing and sweating steps under the optimal conditions (PNDf) is easy and can produce pure water in cold and remote regions. The process led to a frozen film salinity less than 0.4 g/kg after 29 h. In addition, the TDS in the Fao seawater was reduced by 79% and drinking water was produced in one step. However, the energy consumption of the PNDf process is high; thus, PNDf is a simple process but requires development to reduce the energy consumption.

References

- [1] A. Madani, Economics of desalination for three plant sizes, *Desalination*, 78 (1990) 187–200.
- [2] A. Madani, S.E. Aly, A combined RO/freezing system to reduce inland rejected brine, *Desalination*, 75 (1989) 241–258.
- [3] O. Miyawaki, L. Liu, Y. Shirai, S. Sakashita, K. Kagitani, Tubular ice system for scale-up of progressive freeze-concentration, *J. Food Eng.*, 69 (2005) 107–113.
- [4] M.V. Rane, Y.S. Padiya, Heat pump operated freeze concentration system with tubular heat exchanger for seawater desalination, *Energy Sustain. Dev.*, 15 (2011) 184–191.
- [5] W. Rice, D.S.C. Chau, Freeze desalination using hydraulic refrigerant compressors, *Desalination*, 109 (1997) 157–164.
- [6] J. Sánchez, E. Hernández, J.M. Auleda, M. Raventós, Freeze concentration of whey in a falling-film based pilot plant: process and characterization, *J. Food Eng.*, 103 (2011) 147–155.
- [7] J. Sánchez, Y. Ruiz, M. Raventós, J.M. Auleda, E. Hernández, Progressive freeze concentration of orange juice in a pilot plant falling film, *Innov. Food Sci. Emerging Technol.*, 11 (2010) 644–651.
- [8] G.L. Stepakoff, D. Siegelman, R. Johnson, W. Gibson, Development of a eutectic freezing process for brine disposal, *Desalination*, 15 (1974) 25–38.
- [9] W. Gao, D.W. Smith, D.C. Sego, Freezing behavior of freely suspended industrial wastewater droplets, *Cold Reg. Sci. Technol.*, 31 (2000) 13–26.
- [10] G. Gay, O. Lorain, A. Azouni, Y. Aurelle, Wastewater treatment by radial freezing with stirring effects, *Water Res.*, 37 (2003) 2520–2524.
- [11] W. Gao, M. Habib, D.W. Smith, Removal of organic contaminants and toxicity from industrial effluents using freezing processes, *Desalination*, 245 (2009) 108–119.
- [12] P. Ganorkar, A. Nandane, A. Tapre, Reverse Osmosis for Fruit Juice Concentration – A Review, *J. Food Sci. Technol.*, 1 (2012) 23–36.
- [13] X. Cheng, M. Zhang, B. Xu, B. Adhikari, J. Sun, The principles of ultrasound and its application in freezing related processes of food materials, *Ultrason. Sonochem.*, 27 (2015) 576–585.
- [14] M.A. Darwish, M. Abdel-Jawad, J. Leif, A new dual-function device for optimal energy recovery and pumping for all capacities of RO systems, *Desalination*, 75 (1989) 25–39.
- [15] H. Mohammed, I. Dore, Forecasting the economic costs of desalination technology, *Desalination*, 172 (2005) 207–214.
- [16] N. Yazdanpanah, A. Myerson, B. Trout, Mathematical modeling of layer crystallization on a cold column with recirculation, *Ind. Eng. Chem. Res.*, 55 (2016) 5019–5029.

- [17] APHA, Standard Methods for the Examination of Water and Wastewater, American Public Health Association, American Water Works Association and Water Environment Federation, Washington, D.C., USA, 1998.
- [18] L. Vrbka, P. Jungwirth, Brine rejection from freezing salt solutions: a molecular dynamics study, *Phys. Rev. Lett.*, 95 (2005) 148501.
- [19] P. Wang, T.S. Chung, A conceptual demonstration of freeze desalination-membrane distillation (FD-MD) hybrid desalination process utilizing liquefied natural gas (LNG) cold energy, *Water Res.*, 46 (2012) 4037–4052.
- [20] D. Zhou, L. Zhu, Y. Fu, M. Zhu, L. Xue, Development of lower cost seawater desalination processes using nanofiltration technologies – a review, *Desalination*, 376 (2015) 109–116.
- [21] J. Chang, J. Zuo, K.J. Lu, T.S. Chung, Freeze desalination of seawater using LNG cold energy, *Water Res.*, 102 (2016) 282–293.
- [22] R. Singh, Sustainable fuel cell integrated membrane desalination systems, *Desalination*, 227 (2008) 14–33.
- [23] Y. Hui, Z. Zhonglai, Y. Yuexin, Influence of gravity-induced brine drainage on seawater ice desalination, *Desalination*, 407 (2017) 33–40.
- [24] M.A. Darwish, S. Alotaibi, S. Alfahad, On the reduction of desalting energy and its cost in Kuwait, *Desalination*, 220 (2008) 483–495.
- [25] M. Himmelblau, *Process Analysis by Statistical Methods*, Wiley, New York, 1970.